# The ribosome revealed

Rachel Green and Joseph D. Puglisi

**Several recently reported structures reveal the details of ribosome architecture and provide new insights into the mechanism of protein synthesis.**



The ribosome is the two-subunit ribonucleoprotein particle that translates the genetic material into an encoded polypeptide. The two subunits have distinct functions: the small subunit (30S in bacteria) is the site of the codon–anticodon interaction between the messenger RNA (mRNA) and the transfer RNA (tRNA) substrates, and the large (50S) subunit catalyzes peptide bond formation. The two subunits interact intimately in the 70S particle to coordinate these events and to translocate to the next codon on the mRNA (Fig. 1). Electron microscopy has identified the gross morphological features of ribosomal particles, and single particle cryo-electron microscopy (cryoEM) has revealed a higher resolution view (15 Å) of ribosomes in the presence of tRNAs and protein factors[1]. Advances in the crystallography of ribosomes have promised an atomic level view of the ribosome. Recently, landmark structures of the 30S and 50S subunits at between 4.5 and 5.5 Å resolution (refs 2,3; A. Yonath, pers. comm.) and the 70S ribosome at 7.8 Å resolution[4] have begun to deliver on this promise (Fig. 2), and to provide new insights into ribosome function. In the end, each of these studies has a different focus, thus providing us with detailed information on a number of functional domains. Here we give an overview of the details of these new structuress, whetting our appetites for the atomic resolution structures to come.

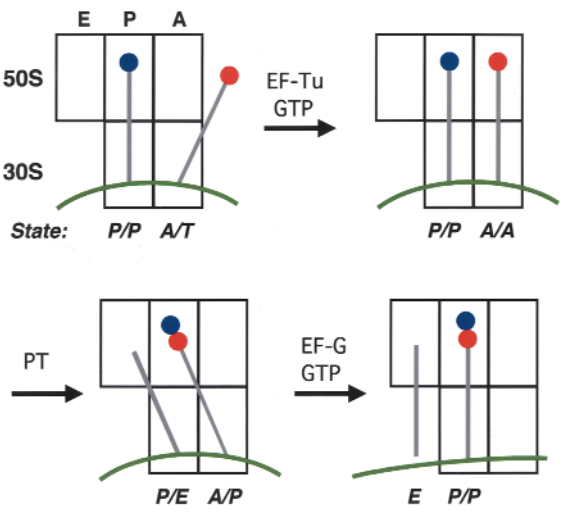


**Fig. 1** Hybrid states model for the translational elongation cycle[55]. tRNA binding sites on the 50S and 30S subunits are represented schematically by upper and lower rectangles, respectively. The 50S subunit is divided into A (aminoacyl), P (peptidyl) and E (exit) sites; the 30S subunit is subdivided into A and P sites. tRNAs are represented by vertical bars and amino acids by small colored circles. mRNA is represented as a green line bound to the 30S subunit. The directional movement of the acylated and deacylated tRNAs through the ribosome, catalyzed by elongation factors EF-Tu and EF-G, during the translational cycle is indicated. PT stands for peptidyl transfer.

Although high quality diffracting crystals of the ribosome have been available for a number of years[5,6], the technical 'phase' problem associated with the large and asymmetric ribosome was finally overcome by combining standard methods with high power synchrotron radiation. This was no simple task, as the ribosome and its subunits represent the largest asymmetric structures solved by X-ray crystallography. Now, for the first time, double stranded RNA helices and the α-helices of ribosomal proteins are readily identified leading to exact placement of a substantial number of ribosomal proteins and RNA domains within the ribosomal particles. The resolution of the subunit structures at ~5 Å is sufficient for the placement of previously solved protein and RNA structures and those elements for which there is considerable biochemical information linking them to known structures. However, the resolution is not sufficient to directly trace the phosphodiester backbone of the RNA chain or to solve unknown protein structures. Thus, the interpretations of these partial ribosome structures were only possible in the context of the vast biochemical and genetic database of the ribosome field.

The 30S subunit is composed of one large rRNA (16S in *Escherichia coli* is 1,542 nucleotides (nt) long) and ~20 proteins and has been the focus of exhaustive biochemical, genetic and structural analysis for several decades. The 16S rRNA can be divided into domains — the 5' domain, the central domain, the 3' major and the 3'minor domains (the penultimate stem) — which have been, in turn, roughly assigned to the body, the platform, the head and the cleft of the subunit, respectively (Fig. 2*a*). The relative placement of each of the 21 proteins (of *E. coli*) within the 30S particle was possible by making use of the neutron scattering studies[7], and the crystal or NMR structures of seven previously determined 30S subunit proteins[8].

In two studies, Clemons *et al.*[3] present a 5.5 Å structure and Yonath and colleagues (pers. comm.) present a 4.5 Å structure of the eubacterial *Thermus thermophilus* 30S subunit. In the structure presented by Yonath and coworkers (pers. comm.), the resolution is high, resulting in a striking view of the subunit. A long RNA helix on the subunit interface is proposed to be the penultimate stem of 16S rRNA (helix 44), although the individual nucleotide bases cannot yet be distinguished. The use of a mercurated cDNA oligonucleotide probe complementary to the 3' end of 16S rRNA (acting as a Shine-Dalgarno motif in an mRNA) allowed for placement of the anti-Shine-Dalgarno sequence in the platform of the subunit. In addition, the known structures of the S5 and S7 proteins were fit into the electron density. Although few of the components of this 30S subunit have been placed, the high resolution of this structure foreshadows the type of detailed information that will

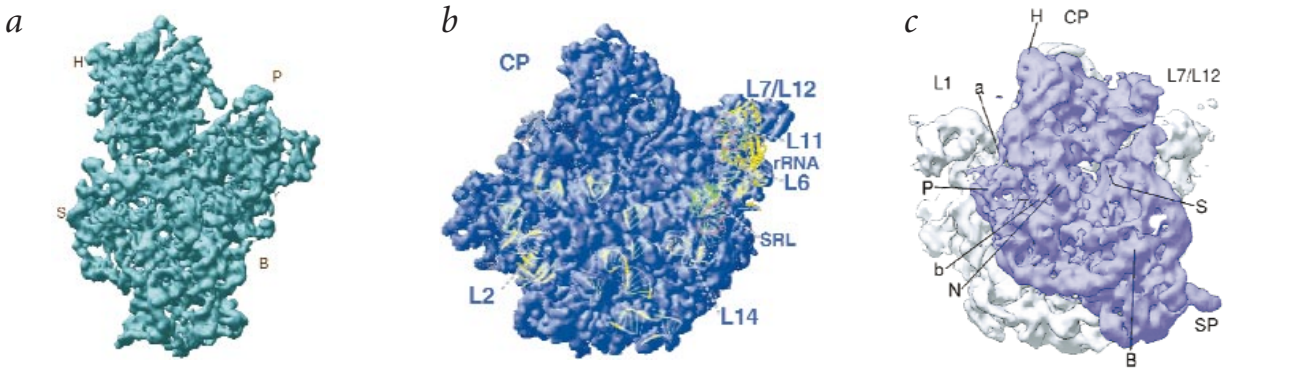


**Fig. 2** Electron density maps of the 30S, 50S and 70S ribosomal particles. ***a***, *Thermus thermophilus* 30S subunit at 5.5 Å resolution[3]. The intersubunit interface points towards the viewer. The head (H), platform (P), shoulder (S) and body (B) are indicated. ***b***, *Haloarcula marismortui* 50S ribosomal subunit at 5 Å resolution[2]. The subunit interface points towards the reader. RNA regions that have been fit are in yellow. The central protuberance (CP) is indicated, as are the proteins and RNA that have been specifically fit to the density. ***c***, *Thermus thermophilus* 70S subunit at 7.8 Å resolution[4]. The 30S subunit is in blue and 50S subunit is white. The head (H), platform (P), body (B), spur (SP) and shoulder (S) are indicated, as are contacts between the head and platform (a and b). Proteins L1 and L7/12 regions on the 50S subunit are indicated.



be obtained ultimately from atomic resolution structures.

In the 5.5 Å structure presented by Clemons *et al.*[3] (Fig. 2*a*), the resolution is somewhat lower, but the number of ribosomal components that have been fit to the electron density, some of them perhaps only tentatively, is remarkable. The 30S proteins (S4, S5, S6, S7, S8, S15 and S17) of known structure[8] were positioned in the electron density and another six proteins (S2, S3, S11, S16, S18 and S20) of unknown structure were placed into regions of α-helical density based on neutron scattering and biochemical data. S20 has been assigned to a three-helix bundle in the bottom of the body of the subunit that is easily traced in the electron density; this placement is consistent with biochemical data but not with neutron scattering data. This assignment represents a low-resolution structure for S20 consistent with secondary structural predictions based on its sequence. Thus, almost two-thirds of the proteins of the small subunit of the ribosome have been assigned, at least tentatively, to regions of electron density in a 5.5 Å map of the subunit. When the assignments of the seven proteins of known structure are compared with the neutron scattering data, there is general agreement when S15 is excluded from this comparison. Placement of S15 on the solvent side of the subunit by neutron scattering conflicts with biochemical data[9,10], and also with structural assignments placing S15 at the interface of the 30S subunit[11].

Tracing of the RNA chains in the electron density maps is difficult at this resolution. First, there are few known structures of rRNA[12–15] that can be fit directly, as with the protein structures. Second, although the connectivity of the RNA secondary structure elements constrains their positions, tracing of the backbone at this resolution is difficult. Undaunted, the authors have assigned approximately one-third of the well-determined 16S rRNA secondary structure to helical regions of the 30S subunit density. The fold of the entire central domain of 16S rRNA (~350 nt) was determined, and the 3' minor domain of 16S rRNA (the penultimate stem) was assigned to the long, protein-free, helical region extending from the cleft of the subunit down the body at the subunit interface (Fig. 3*a*). This stem, isolated at the interface of the subunit, beautifully reveals two strands of RNA, the major and minor grooves of the RNA helix and the bumps associated with the density of the phosphate groups.

The central domain of 16S rRNA and its associated proteins form the platform and parts of the body of the 30S subunit. The platform has conformational flexibility with respect to other domains of the subunit, which may be correlated to the structural movements of translation[16–18]. Nucleotide numbering refers to the rRNA sequence in *E. coli*, whereas helix numbering is sequential in the well-established 16S rRNA secondary structure. The central domain of 16S rRNA contains the 690 and 790 (H23, H24) stem-loop regions that have been implicated in subunit association (and as potential bridging components)[19,20] and the helical region H27 (900 loop) that has been implicated in a conformational switch essential to the decoding function of the 30S subunit[21]. Further, there is considerable biochemical data regarding the interaction between the S8 and S15 proteins and their 16S rRNA binding sites[22–25].

The central domain rRNA was fit independently of the ribosomal proteins into the electron density map of the subunit. When the RNA and protein fits were merged, both RNA–RNA and RNA–protein interactions were evident, highlighting the extent to which the various elements of the ribosome are integrated. The minor grooves of the 690 and 790 loops of 16S rRNA extend from the platform into the subunit interface poised for functional interaction with the 50S subunit[4] (Fig. 3*a*). The known role of H27 in accuracy is consistent with its location proximal to S5 (ref. 21) and its intimate association with the penultimate stem (H44) near the A-site decoding region. These relative locations suggest that translational accuracy may be modulated by structurally coupled movements of the decoding site and H27 rRNA elements. Previously identified *ram* mutations in ribosomal proteins S4 and S5 (refs 26,27), which decrease translational accuracy, occur on the protein–protein interface between these two molecules. Direct RNA–protein interactions are observed in many places — for example, proteins S8 and S15 and the RNA core of the central domain (the three-way junction between H20-H21-H22) form extensive interactions to stabilize its structure.

Perhaps the most striking feature of the 30S subunit structure is the absence of proteins from the subunit interface[4] (Fig. 3). This RNA-rich interface must modulate interaction between the two subunits and the movement of tRNAs through this channel. The extreme conservation in this functional interface region is consistent with the fact that the 40S subunit of the eukaryote *Artemia salina* can be combined in a functional ribosomal particle with the 50S subunit of the bacterium *E. coli*[28,29]. The fact that this functionally critical interface is predominantly RNA supports the notion that ribosomes were once RNA-only machines.

The 50S subunit of the ribosome is composed of two RNAs (5S in *E. coli* is 120 nt and 23S is 2,904 nt) and ~30 proteins. Because of its size and complexity, the 50S subunit has presented a more formidable barrier to experimental analysis. The reconstitution of 50S subunits from the individual RNA and protein components is difficult[30], hindering structural and biochemical analyses that were performed on the 30S subunit. Further, there are incomplete neutron scattering and biochemical data to position the more than 30 proteins[31]. There are, however, considerable biochemical data on the peptidyl transferase region that binds the 3' ends of tRNAs and on the factor binding center (GTPase center) where elongation, initiation and release factors interact and initiate their various translational processes. High resolution structures have been determined for 10 different large subunit proteins[8,32], two RNA fragments (the sarcin-ricin loop and 5S rRNA)[33–36], and two different RNA–protein structures (L11 complexed with its 23S rRNA binding site[37,38] and L25 complexed with a fragment of 5S rRNA; M. Lu and T.A. Steitz, unpublished results).

Ban *et al.*[2] present a 5 Å resolution X-ray structure of the 50S subunit of the archaebacterium *Haloarcula marismortui*. In the 50S structure there are deep crevices and open spaces that appear to separate large structural domains. The extent to which these domains are flexible, allowing the movements required for translation, remains unknown. Some of the crevices and channels that appear in the 50S subunit have a clear role in translation. Peptidyl transfer must occur in a solvent-protected region of the ribosome to prevent premature hydrolysis of the precious peptidyl tRNA; the deep cleft below the central protuberance provides such an environment. Similarly, a channel is observed that connects the site where cryo-EM structures placed the acceptor end of fMet-tRNA$^{fMet}$ in the P site[39] to the site where the central pore of the Sec61 complex binds to yeast ribosomes[40]. This site must represent the exit channel for newly synthesized peptides. Remarkably, in the heavy atom derivatives of Ban *et al.*[2], four different tungsten clusters align in the contours of this channel, defining its outer dimensions at ~20 Å (Fig. 4). Thus, even at a resolution of 5 Å, details of the ribosomal structure that reflect on its function are emerging.

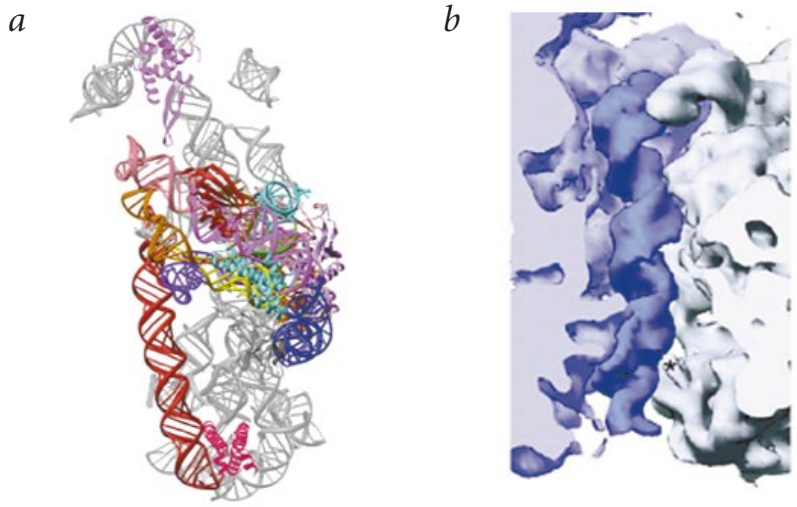


**Fig. 3** The subunit interface between 30S and 50S particles is rich in RNA. ***a***, Side view of the 30S subunit structure[3] with the fit RNA elements shown. The subunit interface is to the left. ***b***, The long penultimate stem is the site of many intersubunit contacts in the 70S ribosome[4]. The 30S subunit is blue, the 50S subunit is grey, and penultimate stem is highlighted in dark blue.

As in the structures of the 30S subunit, RNA helices are readily distinguished in this 5 Å structure, including a prominent helix that extends along the rim of the deep cleft where the peptidyl transferase reaction occurs. The authors speculate that this long helical element is composed of a number of stacked short helices emanating from different regions of the 23S rRNA. In other areas, RNA helices are seen lying side by side, recalling the ribose zippers observed in the crystal structure of the P4–P6 domain of the group I intron[41]. Other specific RNA motifs are also seen including GNRA tetraloops and a backbone S-turn that identified for these authors the previously solved sarcin-ricin loop (SRL) found in domain VI of 23S rRNA[33,34].

Finally, α-helices of proteins are readily distinguished, often allowing for the more difficult placement of associated β-sheets. In this structure, 12 different proteins have been located and the atomic coordinates of five proteins (L1, L2, L6, L11 and L14) have been fitted to the density. In general, these proteins are dispersed throughout RNA-containing regions and appear to form interactions with multiple regions of the rRNA — acting as structural linchpins to orient the RNA domains with respect to one another. The relative lack of biochemical data on many large subunit proteins certainly hinders the fitting at this resolution. Notably, while the RNAs of the archael and eubacterial ribosomes are quite homologous, some of the ribosomal proteins bear homology but others do not. Thus, caution should be exercised when comparing this higher resolution 50S structure to that of the bacterial 70S structure.

The focus of the 50S structure is the placement of RNA and protein components found in the factor binding center — one of the most functionally interesting regions of the large subunit responsible for productive interactions with the GTP motor proteins of the ribosome. Ban *et al.*[2] used the following approach. They first identified the location of the SRL RNA. Then the proteins L6, L11 and L14 proximal to the RNA elements (the SRL and the 1070 and 1100 helices in of 23S rRNA) were fit into the electron density at the base of the L7/L12 stalk region. This region has been implicated in interactions with these proteins and with the elongation factors of translation. In the map, there is no electron density for the N-terminal domain of L11 or for the L7/L12 stalk,

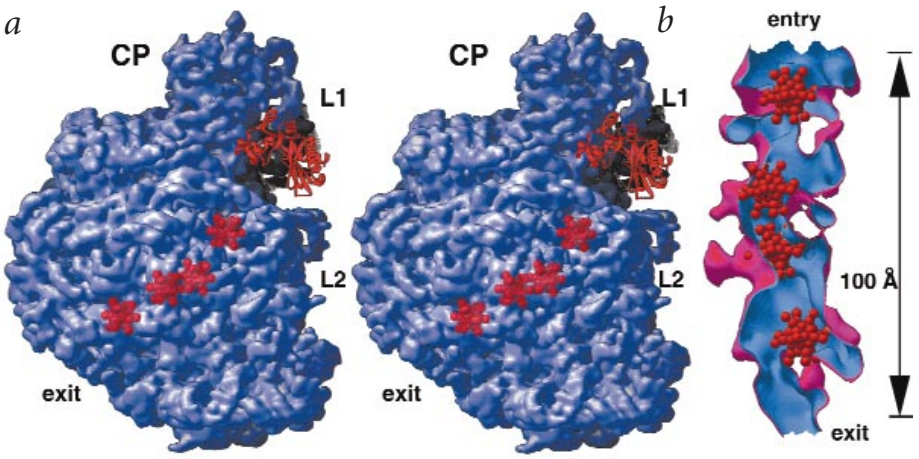


**Fig. 4** ***a***, The tunnel in the 50S ribosomal subunit, with the location of tungsten clusers highlighted. ***b***, Cutaway view of the electron density, showing the empty space within the tunnel.

consistent with a dynamic role for this region in translation.

With a structure of the factor binding center containing the three proteins (L6, L11 and L14) and the two critical RNA components (SRL and the 1070–1100 region of 23S rRNA), the authors modeled the position of EF-G and EF-Tu, based on a consideration of previous low-resolution cryo-EM structures[16,42] and existing biochemical data[43]. The resulting model satisfies many of the predictions of biochemistry although the direct interactions between the 1070–1100 region of 23S rRNA and EF-G indicated by biochemical studies[44,45] are not seen. These discrepancies might be rationalized by the fact that the structure of the 50S subunit presented by Ban *et al.*[2] does not include interactions with the 30S subunit, the substrates or factors of translation. It is easy to imagine that critical structural changes might occur in this region of the large subunit in functional complexes of the ribosome.

Cate *et al.*[4] present the structure of the *T. thermophilus* 70S ribosome at 7.8 Å resolution (Fig. 2*c*), complexed with a short defined mRNA and tRNA ligands. Despite the lower resolution of this structure relative to those of the individual subunits, it provides the most detailed view to date of how the ribosome binds its tRNA substrates and how the two subunits interact. A number of bridges of electron density are observed between the subunits composed of both RNA and proteins. The authors have used biochemical data to help interpret the electron density maps to assign the 690 and 790 helices and 900 loop as RNA components of several specific 30S subunit bridges. In another example, a protein in the 30S subunit (S15) that is involved in an intersubunit bridge with the 700 region of 23S rRNA in the 50S subunit is identified[11]. Finally, the intersubunit interface is dominated on the 30S subunit by the long (100 Å) penultimate stem (helix 44), in agreement with biochemical data and the structures of Clemons *et al.*[3] and Yonath and coworkers (pers. comm.). The total surface area buried in the subunit interface contacts is ~2,100 Å$^2$ in this ribosomal structure. Intriguingly, this buried area represents less than that found in a partial structure (160 nt in length) of the group I intron RNA[41]. This finding is consistent with the the idea the subunit interface region is loosely engaged to facilitate the translocation movements of the ribosome during translation.

The centerpiece of the 70S ribosome structure is the characterization of the tRNA binding sites obtained by cocrystallization of the 70S ribosome with mRNA and either full length tRNAs or anticodon stem-loop mimics of tRNAs (Fig. 5). Using difference methods, the binding sites for P-site and A-site tRNAs have been localized to the same general regions of the ribosome as prior EM studies[46,47], although here the A-site and P-site tRNAs are oriented nearly parallel with respect to one another (Fig. 5, P-site tRNA is blue and A-site tRNA is green) The best data is obtained for the high affinity P-site complex of a tRNA stem loop analog with mRNA and the ribosome. The codon–anticodon interaction of P-site tRNA occurs within a tight cleft on the 30S subunit. Several fingers of ribosome electron density are seen to contact the tRNA anticodon and mRNA, stabilizing their interaction with the ribosome to maintain reading frame and to prevent loss of the peptidyl tRNA during translation. The identity of these contacts remains unknown, but they occur near nucleotides implicated in P-site function[48]. Interestingly, C74 in the 3' end of tRNA is well ordered (though C75 and A76 are apparently not), consistent with the proposed base

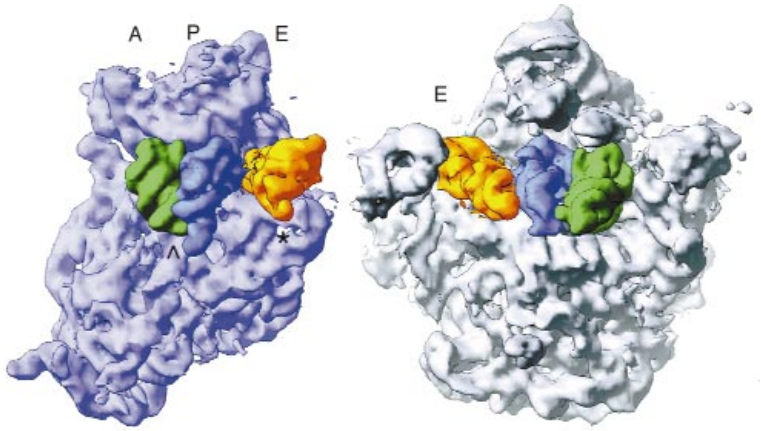


**Fig. 5** Model for transfer RNAs bound to the 70S ribosome, as determined by difference maps in the 70S structure. A-site (green), P-site (dark blue) and E-site (yellow) tRNAs are indicated, and their binding sites on the 30S subunit (blue) and 50S subunit (grey) are shown.

pair of this nucleotide with G2252 in ribosomal RNA[49]. Again, the details of this critical interaction for peptide bond formation await higher resolution (Fig. 5, green tRNA).

The A-site tRNA (Fig. 5, green tRNA), which decodes genetic information via discrimination between cognate and noncognate mRNA codons, binds within a more open pocket on the 30S subunit, near the end of the 16S rRNA penultimate stem. E-site tRNA (Fig. 5, yellow tRNA) density, obtained serendipitously from tRNA contamination in the ribosome preparation, was seen to make close contacts with the ribosome in three regions: the 3'-CCA end of the tRNA in a cleft between the L1 stalk and the central protuberance, the T loop with protein L1 and the anticodon loop in the small subunit cleft between the platform and head. The 900 loop (H27) and helix of the 16S rRNA are proposed to contact the penultimate stem (H44), near the conserved A1413-G1487 pair; the reactivity of these nucleotides to chemical probes is known to be affected by tRNAs, 50S subunits and miscoding agents[50,51]. The authors suggest that RNA conformational changes involving contacts between the penultimate stem and the 900 region could provide signals at the subunit interface that are transmitted to the 50S subunit[3] (Fig. 3*b*). These predictions underline the dynamic nature of the translational machinery and the extent to which intersubunit crosstalk must be at the heart of translation[52,53].

Ribosomes were first visualized in electron micrographs in 1943 (ref. 54) and the basic steps of translation were defined in the 1960's. The next four decades witnessed tremendous advances in our understanding of the ribosome using biochemical, genetic and low resolution structural approaches. The crystallographic studies reviewed here, though not yet at atomic resolution, provide an unprecedented view of ribosomal structure and foreshadow the questions that will be answered and raised when all of the rRNA and ribosomal proteins have been placed into high resolution structures. Already, themes are emerging. RNAs are clearly critical components of functional centers, as suggested by many biochemical results. However, proteins not only stabilize RNA architecture, but may be more directly involved in ribosomal processes, as illustrated by the *ram* mutations in the 30S subunit and the proteins at the factor binding center and subunit interface. In short, the RNAs and proteins of ribosomal particles are inseparable for the myriad functions of translation. The ribosome is a dynamic machine, and the mechanism of translation will only be revealed by kinetic investigations of translation coupled with structural studies of 70S ribosomes with mRNA, tRNAs and initiation, elongation and release factors bound at various steps in the translational cycle. The structures presented this year represent a bold step towards this goal.

*Rachel Green is in the Department of Molecular Biology and Genetics, Johns Hopkins University School of Medicine, Baltimore, Maryland 21205, USA. Joseph D. Puglisi is in the Department of Structural Biology, Stanford University School of Medicine, Stanford, California 94305-5126, USA.*

*Correspondence should be addressed to R.G. email: ragreen@jhmi.edu or to J.D.P. puglisi@stanford.edu.*

1. Agrawal, R.K. & Frank, J. *Curr. Opin. Struct. Biol.* **9**, 215–221 (1999).
2. Ban, N. *et al. Nature* **400**, 841–847 (1999).
3. Clemons, W.M., Jr. *et al. Nature* **400**, 833-840 (1999).
4. Cate, J.H., Yusupov, M.M., Yusupova, G.Z., Earnest, T.N. & Noller, H.F. *Science* **285**, 2095-2104 (1999).
5. Yonath, A. *et al. Acta. Crystallogr. A* **54**, 945-955 (1998).
6. von Bohlen, K. *et al. J. Mol. Biol.* **222**, 11-15 (1991).
7. Capel, M.S. *et al. Science* **238**, 1403-1406 (1987).
8. Ramakrishnan, V. & White, S.W. *Trends in Biochemical Sciences* **23**, 208-213 (1998).
9. Abdurashidova, G.G., Tsvetkova, E.A., Chernyi, A.A., Kaminir, L.B. & Budowsky, E.I. *FEBS Lett.* **185**, 291-294 (1985).
10. Champney, W.S. *Biochim. Biophys. Acta.* **609**, 464-474 (1980).
11. Culver, G.M., Cate, J.H., Yusupova, G.Z., Yusupov, M.M. & Noller, H.F. *Science* **285**, 2133-2136 (1999).
12. Fourmy, D., Recht, M.I., Blanchard, S.C. & Puglisi, J.D. *Science* **274**, 1367-1371 (1996).
13. Puglisi, E.V., Green, R., Noller, H.F. & Puglisi, J.D. *Nature Struct. Biol.* **4**, 775-778 (1997).
14. Kalurachchi, K. & Nikonowicz, E.P. *J. Mol. Biol.* **280**, 639-654 (1998).
15. Butcher, S.E., Dieckmann, T. & Feigon, J. *J. Mol. Biol.* **268**, 348-358 (1997).
16. Agrawal, R.K., Penczek, P., Grassucci, R.A. & Frank, J. *Proc. Natl. Acad. Sci. USA* **95**, 6134-6138 (1998).
17. McCutcheon, J.P. *et al. Proc. Natl. Acad. Sci. USA* **96**, 4301-4306 (1999).
18. Agrawal, R.K., Lata, R.K. & Frank, J. *Int J Biochem Cell Biol.* **31**, 243-254 (1999).
19. Merryman, C., Moazed, D., McWhirter, J. & Noller, H.F. *J. Mol. Biol.* **285**, 97-105 (1999).
20. Lee, K., Varma, S., SantaLucia, J., Jr. & Cunningham, P.R. *J. Mol. Biol.* **269**, 732-743 (1997).
21. Lodmell, J.S. & Dahlberg, A.E. *Science* **277**, 1262-1267 (1997).
22. Serganov, A.A. *et al. RNA* **2**, 1124-1138 (1996).
23. Wu, H., Jiang, L. & Zimmermann, R.A. *Nucleic Acids Res.* **22**, 1687-1695 (1994).
24. Moine, H., Cachia, C., Westhof, E., Ehresmann, B. & Ehresmann, C. *RNA* **3**, 255–268 (1997).
25. Batey, R.T. & Williamson, J.R. *J. Mol. Biol.* **261**, 536–549 (1996).
26. van Acken, U. *Mol. Gen. Genet.***140**, 61–68 (1975).
27. Wittmann-Liebold, B. & Greuer, B. *FEBS Lett* **95**, 91–98 (1978).
28. Klein, H.A. & Ochoa, S. *J. Biol. Chem.* **247**, 8122–8128 (1972).
29. Boublik, M., Wydro, R.M., Hellmann, W. & Jenkins, F. *J Supramol. Struct.* **10**, 397–404 (1979).
30. Nierhaus, K.H. & Dohme, F. *Proc. Natl. Acad. Sci. USA* **71**, 4713–4717 (1974).
31. May, R.P., Nowotny, V., Nowotny, P., Voss, H. & Nierhaus, K.H. *EMBO J.* **11**, 373–378 (1992).
32. Nakagawa, A. *et al. EMBO J.* **18**, 1459–1467 (1999).
33. Szewczak, A.A. & Moore, P.B. *J. Mol. Biol.* **247**, 81–98 (1995).
34. Correll, C.C. *et al. Proc. Natl. Acad. Sci. USA* **95**, 13436–13441 (1998).
35. Correll, C.C., Freeborn, B., Moore, P. B. & Steitz, T. A. *Cell* **91**, 705–712 (1997).
36. Dallas, A. & Moore, P.B. *Structure* **5**, 1639–1653 (1997).
37. Wimberly, B.T., Guymon, R., McCutcheon, J.P., White, S.W. & Ramakrishnan, V. *Cell* **97**, 491–502 (1999).
38. Conn, G.L., Draper, D.E., Lattman, E.E. & Gittis, A.G. *Science* **284**, 1171–1174 (1999).
39. Malhotra, A. *et al. J. Mol. Biol.* **280**, 103–116 (1998).
40. Beckmann, R. *et al. Science* **278**, 2123–2126 (1997).
41. Cate, J.H. *et al. Science* **273**, 1678–1685 (1996).
42. Stark, H. *et al. Nature* **389**, 403–406 (1997).
43. Wilson, K.S. & Noller, H.F. *Cell* **92**, 131–139 (1998).
44. Moazed, D., Robertson, J.M. & Noller, H.F. *Nature* **334**, 362–364 (1988).
45. Skold, S.E. *Nucleic Acids Res.* **11**, 4923–4932 (1983).
46. Stark, H. *et al. Cell* **88**, 19–28 (1997).
47. Agrawal, R.K. *et al. Science* **271**, 1000–1002 (1996).
48. Prince, J.B., Taylor, B.H., Thurlow, D.L., Ofengand, J. & Zimmermann, R.A. *Proc. Natl. Acad. Sci. USA* **79**, 5450–5454 (1982).
49. Samaha, R.R., Green, R. & Noller, H.F. *Nature* **377**, 309–314 (1995).
50. Moazed, D. & Noller, H.F. *Nature* **327**, 389–394 (1987).
51. Moazed, D. & Noller, H.F. *Cell* **47**, 985–994 (1986).
52. O'Connor, M. & Dahlberg, A.E. *J. Mol. Biol.* **254**, 838–847 (1995).
53. Mitchell, P., Osswald, M. & Brimacombe, R. *Biochemistry* **31**, 3004–3011 (1992).
54. Luria, S.E., Delbruck, M. & Anderson, T.F. *J. Bact.* **46**, 57 (1943).
55. Moazed, D. & Noller, H.F. *Nature* **342**, 142–148 (1989).